

Quantitative depth profiles of vacancy cluster defects produced by MeV ion implantation in Si: Species and dose dependence

R.Kalyanaraman, T.E.Haynes

Solid State Division, Oak Ridge National Laboratory, Oak Ridge, TN 37831

D.C.Jacobson, H.-J.Gossmann, and C.S.Rafferty

Lucent Technologies, Bell Laboratories, Murray Hill, NJ 07974

ABSTRACT

Monte Carlo simulation codes such as TRIM or MARLOWE show a net displacement of interstitials with respect to vacancies from the Frenkel pairs produced in implant cascades. As a result, defect profiles after recombination have an excess of vacancies (V^{ex}) in the shallow region of these implants, with excess interstitials near the projected range R_p . Typically, accurate estimates of the V^{ex} distribution are computer intensive as the complete history of each damage cascade must be recorded. In this work we introduce a method for fast estimation of the V^{ex} profile based on the derivative of the recoil distribution obtained from binary collision simulations using the Kinchen-Pease approximation for damage production. Also, Au labeling has been used to quantitatively analyze and compare the experimental depth profiles of V^{ex} produced by implants of B, Si, and Ge into Si for a range of doses. Specific conditions like matching of the projected range of the implanted ions and matching of the number of Frenkel pairs created have been compared. This detailed study and comparison with simulation provides the first systematic, quantitative measurements of the V^{ex} concentrations over such a range of species and doses. In analogy to the “+ number” for excess interstitials from ion implantation, we determine the range of “minus (-) numbers”, that is the number of excess vacancies per implanted ion for the different species. For Si it is constant in the dose range studied at -0.05, while for B it is -0.001 to -0.004 and for Ge, -0.1 to -0.2. The general shapes of the V^{ex} profiles are similar to those obtained from simulation. Evidence is presented that one significant difference, namely an experimentally observed vacancy depletion near the surface, may be due to the diffusion and annihilation of vacancies at the surface. In addition, an increased nucleation probability of vacancy defects close to R_p may account for the growth of excess vacancies from close to R_p towards the surface with increasing implant dose.

INTRODUCTION

The study of excess vacancy-type defects arising from processing steps involving high vacancy supersaturation [1] is now entering an exciting phase of study. It has recently been shown that Au labeling can quantitatively measure and profile the concentration of vacancy-type defects [2], i.e. it is now possible to directly compare theory or simulation with experiment. For example, the V^{ex} resulting from momentum transfer of recoiled atoms in damage cascades formed from high-energy ion (HEI) implantation can be simulated using binary-collision codes such as TRIM [3] or MARLOWE [4] and compared with experimental data. In this work we will first discuss an alternative method for estimating the V^{ex} distribution arising in high energy and/or high dose implantation into Si that is faster than complete, full-cascade simulations. Following this a comparison is made between the simulations and experiment for the case of 2 MeV, $1 \times 10^{16} \text{ cm}^{-2} {}^{28}\text{Si}^+$ implantation into p-type float-zone Si(100). Some apparent differences are discussed on the basis of current experimental evidence for vacancy outdiffusion and

trapping near the surface. Finally, the dependence of V^{ex} concentration on implanted species and dose is compared and the range of “- number” is determined for implantation of B, Si, and Ge ions.

EXPERIMENTAL DETAILS

In this work, p-type FZ Si(100) wafers were used for all the studies. High-energy implants of 2 MeV $^{28}\text{Si}^+$ (3×10^{15} - 1×10^{16} cm^{-2}), 3.25 MeV $^{74}\text{Ge}^+$ (7×10^{14} - 2.5×10^{15} cm^{-2}) or 1.2 MeV $^{10}\text{B}^+$ (2×10^{16} - 8.5×10^{16} cm^{-2}) were used to study species and dose dependence of the V^{ex} concentration. Implant temperatures were $\sim 75^\circ\text{C}$ for Si and B and 175°C for Ge in order to avoid amorphization at the highest doses. TRIM simulations using the SRIM version 2000.39³ were used to simulate V^{ex} concentrations. Au labeling [2] was done via a 68-keV, 8×10^{14} cm^{-2} Au implant followed by 750°C anneals in Ar until saturation of Au in the V^{ex} region. Final analysis of the Au profiles was carried out by Rutherford backscattering spectrometry (RBS) using a 2.8 MeV $^4\text{He}^{2+}$ beam at an incident angle of 22° to the normal. All implants and RBS analyses were performed on a 1.7MeV National Electrostatics tandem Pelletron.

DISCUSSION

The V^{ex} profiles from ion implantation can be estimated from Monte-Carlo simulation codes like TRIM or MARLOWE by directly subtracting the depth profiles of recoils and vacancies. Typically the calculations, for e.g. using TRIM, are computer intensive as the history of each damage cascade must be followed and recorded. Furthermore, since the determination of excess defect profiles requires taking a small difference between two much larger numbers, the simulation must be run for large number of ions for statistical validity. Typical run times of a few days and upward (depending on processor speeds) are not uncommon. The V^{ex} distribution arises from the net forward momentum acquired by the recoiled atoms as a result of high energies and/or high doses of implanted ions. As a result of this forward momentum there is a separation in the distribution of the interstitials (I) and vacancies (V) arising from Frenkel pair formation in the damage cascades [5]. This separation gives rise to a local increase in the number of V's with respect to I's in the region from the surface to near the projected range (R_p), while the opposite (i.e. $I > V$) is true for regions near R_p and deeper. In an alternate route to determine this local difference more quickly, we first obtain a net shift (Δz) in the profile of the recoiled atoms with respect to the vacancies by obtaining the difference in projected range (calculated from the first moments of the respective total defect distributions) for each of the two profiles, i.e.

$$\Delta z = R_p^{\text{I}} - R_p^{\text{V}} \quad (1)$$

(superscripts indicate recoiled atoms and vacancies respectively).

This shift is obtained relatively quickly by running a full TRIM simulation for a small number of ions (typically between 500-1000 ions). The V^{ex} profile is then determined from:

$$V^{\text{ex}}(z) = (dR^{\text{KP}}(z)/dz) * \Delta z, \quad (2)$$

where $R^{\text{KP}}(z)$ is the recoil profile determined from the Kinchen-Pease approximation. Figure 1a compares the excess defect profiles for 2 MeV, 1×10^{16} cm^{-2} Si implant determined using Eq. (2)

to that from a full-cascade simulation. As is clearly evident, the derivative method gives results after just 8000 simulated ions that are comparable to the simulations involving full cascades after a lengthy 130,000 ions. The signal-to-noise ratio in the curve from the derivative method can be improved by running a few 100,000 ions using the Kinchin-Pease approximation, which can be run much faster than a comparable number of ions with full cascades.

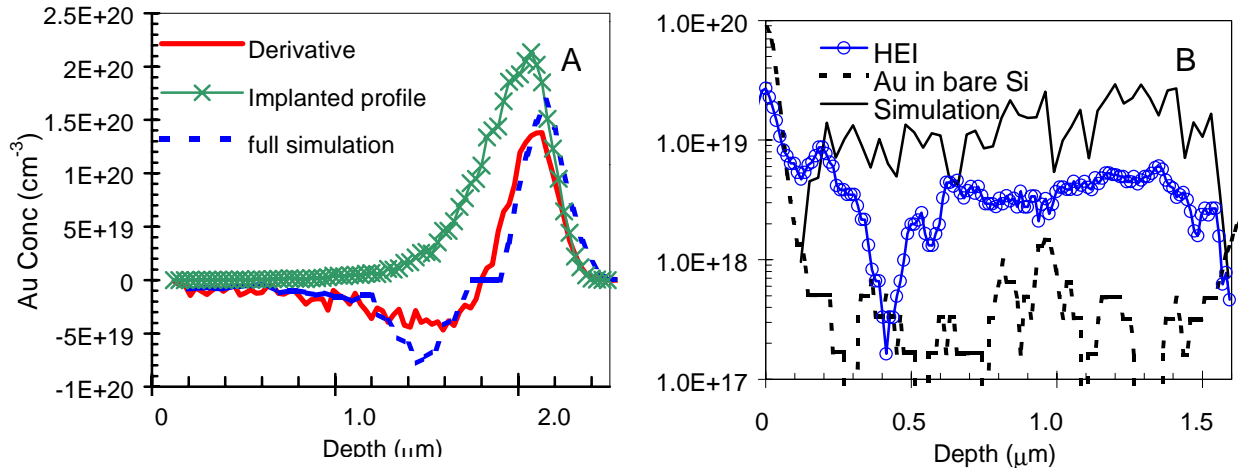


Figure 1. a) V^{ex} profiles from full (dotted line) vs. the derivative method of Eq. (2) (solid line) using SRIM2000. The implanted profile is also shown. b) Comparison of experimentally observed V^{ex} (open circles) with the simulated profile from SRIM (solid line) for a 2 MeV, $1 \times 10^{16} \text{ cm}^{-2}$ Si self-implant. Also shown is the Au profile after drive-in into a bare Si sample (dashed line).

Fig. 1b compares the simulated V^{ex} profile from the derivative method for the 2MeV, 10^{16} cm^{-2} $^{28}\text{Si}^+$ HEI into Si(100) and the experimentally observed profile. The experimental profile was obtained by Au labeling the as-implanted sample for 20 hrs at 750°C to saturate the Au concentration in the V^{ex} region. For the region between 0.5-1.6μm, the shape and magnitude of the simulated and experimental profiles are very similar, although the experimentally observed concentration is a factor of 2 lower than the simulation. The most significant difference occurs in the depth range of 0.3-0.5μm, where the experiment shows a significantly reduced concentration of V^{ex} relative to the simulation. The simulation shows that the theoretical vacancy profile should be relatively constant in the range of 0.3-0.5 μm with a concentration comparable to that at 1 μm. Taking the difference between such a flat profile having the measured peak concentration, and the actual measured profile, we estimate that $\sim 1.5 \times 10^{14} / \text{cm}^2$ vacancies are “missing” between 0.3 and 0.5 μm. The figure also shows the experimentally observed RBS profile for a Si sample with only the Au drive-in. While the HEI sample is accompanied by an additional Au peak labeled the “shoulder” peak, between ~ 0.1 -0.3μm, this is not present for the simulation or in the Si sample with only the Au drive-in. This indicates that the shoulder peak is not a result of Au capture by end-of-range (EOR) defects from the 68-keV Au implant [2] and also that the simulation cannot account for this. Further, the integral of Au in the shoulder peak is comparable in areal density to the missing vacancy concentration defined above. This comparison suggests that the missing vacancies may be escaping to the surface during any post-implant high-temperature steps and may be trapped at the shoulder peak.

Additionally, fig. 2 shows that a medium energy Si implant of 350 keV ($R_p = 0.53\mu\text{m}$) into the V^{ex} region of a 2 MeV, $1 \times 10^{16} \text{ cm}^{-2}$ Si HEI (that had an 815°C , 20 min preanneal in Ar) reduces the amount of Au at the shoulder after subsequent Au labeling. This smooth decrease in concentration at the shoulder with increasing dose of the 350-keV implant indicates that interstitials from the implant are reducing the gettering of Au at the shoulder. Since the shoulder appears only in samples with an MeV implant and is reduced by the injection of additional interstitials, it strongly suggests that the shoulder is due to vacancy-type defects. This effect is consistent with an interstitial-vacancy recombination resulting in a decrease in the concentration of V^{ex} type defects at the shoulder. The details of the trapping of vacancies at the shoulder are currently being investigated.

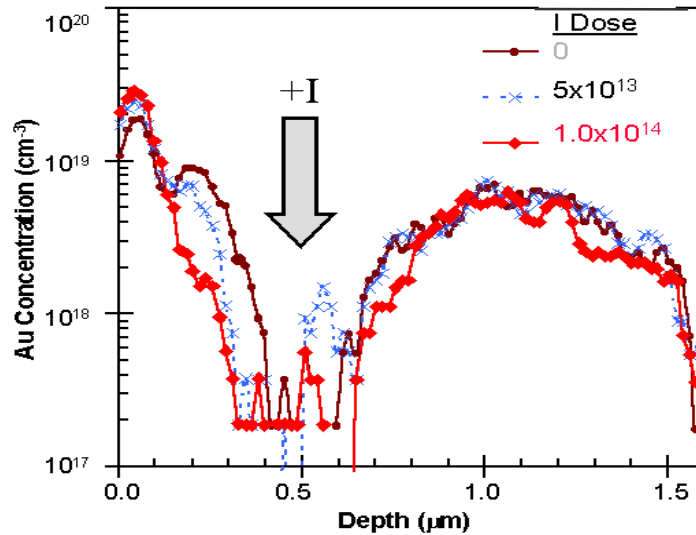


Figure 2. Decrease in Au at shoulder of a HEI sample due to a 350 keV Si implant and anneal following the HEI. The solid arrow indicates the R_p of the 350-keV implant of various doses. The HEI sample without the 350-keV implant is shown in solid circles.

We have also studied the species dependence of B, Si and Ge [6] implants on the formation of V^{ex} . The implant energy for each ion was chosen to match the R_p ($\sim 2\mu\text{m}$) of 2 MeV Si. The nuclear energy deposited by each ion was obtained from TRIM calculations and the dose was scaled such that the total number of Frenkel-pairs produced was similar for all the species. Accordingly, the Ge dose was reduced relative to Si by a factor of 0.25x and the B dose increased by 7x. Fig. 3a shows the dose-dependent behavior for Si in the range of 3×10^{15} - $1 \times 10^{16} \text{ cm}^{-2}$ after Au drive-in till saturation in as-implanted samples. Note that this figure shows the *vacancy* concentration, which is equal to the measured Au concentration multiplied by the calibration factor $k = 1.2$ [2]. The V^{ex} concentration decreases with decreasing dose, primarily in the near-surface half of the V^{ex} profile. A similar effect is seen for the Ge implants (fig. 3b) in the dose range of 7×10^{14} - $2.5 \times 10^{15} \text{ cm}^{-2}$ under similar experimental conditions. Also, the V^{ex} profiles are very similar for Si and Ge. This indicates that the net effect of damage production and recombination produces similar V^{ex} profiles for Si and Ge when the doses are scaled to produce comparable total Frenkel-pair concentrations. The dose dependence of the experimentally observed profiles however is different from simulation, which predicts a flat, linear increase in concentration with increasing dose. Since the simulation does not account for effects like clustering, ripening, etc. it is believed that the high density of total defects near R_p (at

~1.6 μm in Fig. 3) immediately following the implant results in nucleation of V^{ex} defects which then grow towards the surface with increasing dose.

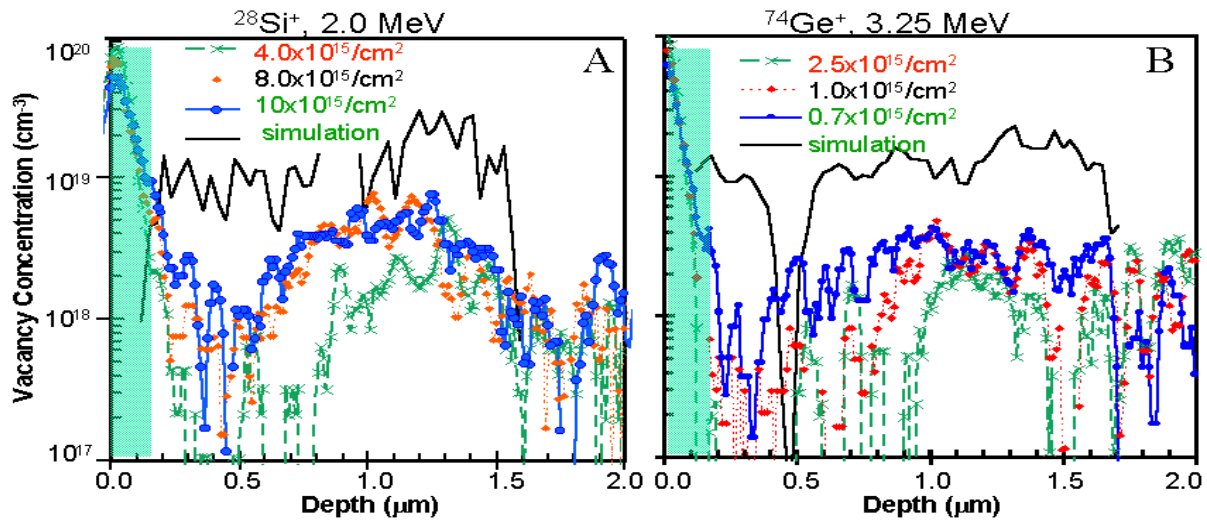


Figure 3. Experimentally observed V^{ex} profiles for Si (fig. 3a) and Ge (fig. 3b) as a function of dose. The V^{ex} curve from SRIM simulation for the highest dose is also shown for comparison. The Au drive-in was carried out in as-implanted samples till saturation.

In fig. 4 is plotted the total integrated V^{ex} for the region between 0.5-1.6 μm for the Si, Ge and B implants. Also plotted in the figure are the theoretical estimates of V^{ex} from SRIM for the same depth window.

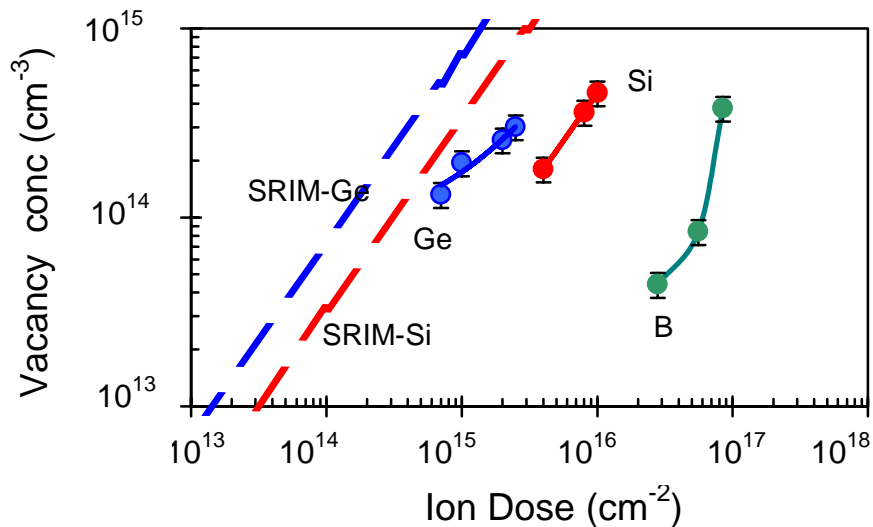


Figure 4. Experimentally observed dose and species dependence of integrated V^{ex} concentration in the $\frac{1}{2}$ Rp region (0.5-1.6 μm). The simulated values for Si and Ge are also shown.

Figure 4 shows that while vacancy cluster concentration after Si implants has a linear dependence on dose, for Ge the dose dependence is sublinear and for B it is superlinear. The “minus number” which is the number of V^{ex} produced per implanted ion is 0.001-0.004 for B, 0.05 for Si and 0.1-0.2 for Ge in the dose range studied. It is clear that a simple scaling of dose from total nuclear energy deposited does not give exactly the same V^{ex} concentrations, especially for light ions such as B, and further studies will be aimed at understanding these differences.

CONCLUSIONS

In summary, we have shown that it is possible to reduce the computation time required to estimate excess defect profiles by using a 2-step “derivative method” which requires: 1) calculating the net shift of the recoiled atoms with respect to vacancies using a few ions in full-cascade simulations and 2) taking the derivative of the recoiled atom profile obtained from faster simulations using the Kinchen-Pease approximation. Further, comparison of theoretically observed curves for 2 MeV, $1 \times 10^{16} \text{ cm}^{-2}$ Si implants with experiment show that for the region between 0.5-1.6 μm , the shapes are similar, with the theory predicting a factor of 2 higher peak concentration of V^{ex} . A distinct difference appears to be in the depletion of V^{ex} to the surface from a depth interval up to $\sim 0.5 \mu\text{m}$ during any subsequent annealing step following the HEI. In many samples, the escaping vacancies appear to be trapped near the surface. The dose-dependent studies clearly show that the evolution of the vacancy-type defects cannot be accounted for by binary collision codes like TRIM and require an understanding of the nucleation and growth of the defects. Furthermore, the species and dose dependence study shows that while the “- number” is constant for Si in the dose range studied it varies for Ge and B in the respective ranges studied.

ACKNOWLEDGEMENTS

Research performed at Oak Ridge National Laboratory was sponsored by the U.S. Department of Energy, Office of Science, Laboratory Technology Research Division and the Division of Materials Sciences under contract DE-AC05-00OR22725 with UT-Battelle, LLC.

REFERENCES

-
1. O.W.Holland, L.Xie, B.Nielsen, D.S.Zhou, J. Elect. Mat. **25**, 99 (1996)
 2. R.Kalyanaraman, T.E.Haynes, V.C.Venezia, D.C.Jacobson, H.-J.Gossmann, and C.S.Rafferty, appearing in App. Phys. Lett. V76, 2000.
 3. J.F.Ziegler, J.P.Biersack, U.Littmark, *The Stopping and Ranges of Ions in Solids*, (pergamon press, New York, 1985).
 4. M.T.Robinson and I.M.Torrens, Phys. Rev. B **9**, 5008 (1974).
 5. A.M.Mazzone, Phys. Stat. Sol. (a) **95**, 149 (1986).
 6. TRIM simulations of As and Ge indicate a nearly 20% mismatch in range for identical energies. This is an unexpected result given the similar masses of the two ions. For this work, SRIM simulations of 3.25 MeV As^+ were used to calculate the damage production, while experiments were performed with 3.25 MeV ^{74}Ge to separate out any chemical effects that could arise from using As.